DILATION AND EROSION OF GRAY IMAGES WITH SPHERICAL MASKS

J. Kukal[1,2], *D. Majerová*[1], *A. Procházka*[2]

[1] CTU in Prague
[2] ICT Prague

Abstract

Any morphological operation with binary or gray image is a time consuming task in the case of large masks (structure elements) that must be applied. The paper is oriented to the application of the fast Fourier transform (FFT) to the dilation and erosion of n-dimensional gray image with the finite number of gray levels. The method is based on gray level image decomposition to binary images, their processing in the Fourier domain, nonlinear thresholding and composition to the final gray image. The main advantage of our method occurs in the case of large spherical masks use in which case the mask approximation in the Fourier domain decreases substantially the discretization error. Our method can be combined with the discrete approximation of large spherical masks which can be evaluated in the Fourier domain as well.

1 Introduction

Basic morphological operations (dilation, erosion, opening, closing) with a small mask do not bring problems of time consumption. Except of rectangular masks (structure element), the time complexity of dilation is proportional to the product of image and mask sizes, which is unacceptable for large masks inside large images. Our method is based on the replacement of the dilation and erosion by modified convolution with a fixed mask. It is possible to use the fast Fourier transform and thus the time complexity of proposed dilation and erosion methods depends only on the image size. The independence of our method on the mask size enables to use large masks for digital dilation and erosion of gray images.

2 Binary Dilation and Erosion via FFT

Let $n \in \mathbb{N}$ be a number of image dimensions (n-D image) and $L \in \mathbb{N}$, $L > 1$ be a number of gray levels ($L = 2$ for the binary image). Let $N_1, N_2, \ldots, N_n > 1$ be image direction ranges, $\mathbb{B} = \{1, 2, \ldots, N_1\} \times \{1, 2, \ldots, N_2\} \times \ldots \times \{1, 2, \ldots, N_n\}$ be an index set of the image, and

$$N = \mathrm{card}(\mathbb{B}) = \prod_{k=1}^{n} N_k$$

be a number of image elements (image size). Thus, the original image can be represented as a function $\mathrm{X} : \mathbb{B} \to \{0, 1, \ldots, L-1\}$. The values of X outside $\mathbb{B}$ are supposed to be zero ones. The mask can be represented as a function $\mathrm{M} : \mathbb{Z}^n \to \{0, 1\}$ satisfying $1 < m < \infty$ where

$$m = \mathrm{card}\{\vec{w} \in \mathbb{Z}^n ;\ \mathrm{M}(\vec{w}) = 1\}$$

is the mask volume (size). It means, the mask is a finite sampling scheme in $\mathbb{Z}^n$ with mask radius

$$r = \max\{||\vec{w}||_\infty ;\ \mathrm{M}(\vec{w}) = 1\} = \max\left\{\max_{k=1,2,\ldots,n} |w_k| ;\ \mathrm{M}(w_1, w_2, \ldots, w_n) = 1\right\} > 0.$$

Let $\vec{u} \in \mathbb{B}$ be an image element. The mask M defines the neighborhood of $\vec{u}$ as a finite set of m points $\vec{v} \in \mathbb{Z}^n$ satisfying $\mathrm{M}(\vec{v} - \vec{u}) = 1$. A list of neighborhood values can be denoted as

$\mathscr{L}(\vec{u}) = (x_1(\vec{u}), x_2(\vec{u}), \ldots, x_m(\vec{u}))$. Then the dilation and erosion of the image X by the mask M are also functions $\mathrm{D}, \mathrm{E} : \mathbb{B} \to \{0, 1, \ldots, L-1\}$ satisfying

$$\mathrm{D}(\vec{u}) = \max\{\mathrm{X}(\vec{v});\ \vec{v} \in \mathbb{Z}^n \ \wedge\ \mathrm{M}(\vec{v} - \vec{u}) = 1\}$$

$$\mathrm{E}(\vec{u}) = \min\{\mathrm{X}(\vec{v});\ \vec{v} \in \mathbb{Z}^n \ \wedge\ \mathrm{M}(\vec{v} - \vec{u}) = 1\}$$

which can be rewritten as

$$\mathrm{D}(\vec{u}) = \max\{x_k(\vec{u});\ 1 \le k \le m\}$$
$$\mathrm{E}(\vec{u}) = \min\{x_k(\vec{u});\ 1 \le k \le m\}$$

for $\vec{u} \in \mathbb{B}$.

Let $*$ be a convolution operator in $\mathbb{Z}^n$. Then the function $\mathrm{Y} : \mathbb{B} \to \mathbb{N}_0$ is defined as

$$\mathrm{Y}(\vec{u}) = (\mathrm{X} * \mathrm{M})(\vec{u})$$

for any $\vec{u} \in \mathbb{B}$. A formal rewriting comes to more clear formula

$$\mathrm{Y}(\vec{u}) = \sum_{k=1}^{m} x_k(\vec{u}).$$

Theorem 1 (binary dilation and erosion)
Let D, E be the dilation and erosion of the image X with the index set $\mathbb{B}$. Let $L = 2$. Let $\mathrm{p} : \{\mathrm{true}, \mathrm{false}\} \to \{0, 1\}$ be a function which realizes a formal transform of logical value to integer one. Then

$$\mathrm{D}(\vec{u}) = \mathrm{p}\left(\mathrm{Y}(\vec{u}) > \frac{1}{2}\right),$$

$$\mathrm{E}(\vec{u}) = \mathrm{p}\left(\mathrm{Y}(\vec{u}) > m - \frac{1}{2}\right)$$

for any $\vec{u} \in \mathbb{B}$ and mask M of size m.

Proof:

(i) When $\mathrm{D}(\vec{u}) = 0$, then $(\forall k = \{1, 2, \ldots, m\})\, x_k(\vec{u}) = 0$. It implies also $\mathrm{Y}(\vec{u}) = 0 \le \frac{1}{2}$.

(ii) When $\mathrm{D}(\vec{u}) = 1$, then $(\exists k = \{1, 2, \ldots, m\})\, x_k(\vec{u}) = 1$. It implies also $\mathrm{Y}_1(\vec{u}) \ge 1 > \frac{1}{2}$.

(iii) When $\mathrm{E}(\vec{u}) = 0$, then $(\exists k = \{1, 2, \ldots, m\})\, x_k(\vec{u}) = 0$. It implies also $\mathrm{Y}(\vec{u}) \le m-1 \le m-\frac{1}{2}$.

(iv) When $\mathrm{E}(\vec{u}) = 1$, then $(\forall k = \{1, 2, \ldots, m\})\, x_k(\vec{u}) = 1$. It implies $\mathrm{Y}_1(\vec{u}) = m > m - \frac{1}{2}$. $\square$

The theorem 1 is useful for numeric realization of fast dilation and erosion of binary images. Supposing that the image direction ranges $N_1, N_2, \ldots, N_n$ are powers of two, we can represent the mask M and image X as arrays of the same size and then perform the n-dimensional convolution via n-dimensional FFT.

Algorithm 1 (binary dilation and erosion):

1. Realize $\mathrm{X}(\vec{u}), \mathrm{M}(\vec{u})$ as arrays.
2. Calculate $\mathcal{X}(\vec{\omega}), \mathcal{M}(\vec{\omega})$ via FFT.
3. Calculate $\mathcal{Y}(\vec{\omega}) = \mathcal{X}(\vec{\omega})\mathcal{M}(\vec{\omega})$.
4. Calculate $\mathrm{Y}(\vec{u})$ via inverse FFT.
5. Calculate $\mathrm{D}(\vec{u}) = \mathrm{p}\left(\mathrm{Y}(\vec{u}) > \frac{1}{2}\right)$.

6. Calculate $\mathrm{E}(\vec{u}) = \mathrm{p}\left(\mathrm{Y}(\vec{u}) > m - \frac{1}{2}\right)$.

The number of operations (multiplications) in the algorithm 1 is then $\mathrm{T}(N) \sim N \log N$ while the number of operations (comparisons) during the traditional dilation is $\mathrm{T}(N, m) \sim N\, m$. It implies that the algorithm 1 is faster than the traditional one for the mask size $m \geq \lambda \log N$ where $\lambda > 0$ is constant. So, the algorithm 1 is useful for binary dilation and erosion with large mask.

3 Gray Dilation and Erosion

According to basic theorems of digital morphology [5, 6], any gray level dilation can be decomposed to the $L-1$ binary tasks. Summarizing the results of binary tasks, the final gray dilation and erosion are obtained. Let X be the gray image with $L > 2$. We decompose it to a sequence of binary images $\mathrm{X}_1, \mathrm{X}_2, \ldots, \mathrm{X}_{L-1}$ according to the rule

$$\mathrm{X}_k(\vec{u}) = \mathrm{cut}(\mathrm{X}(\vec{u}) - (k-1))$$

where the function $\mathrm{cut} : \mathbb{Z} \to \{0, 1\}$ is defined by the formula

$$\mathrm{cut}(s) = \min(1, \max(0, s)).$$

Every binary image X_k is modified by the mask M using the algorithm 1 to obtain the dilation D_k and erosion E_k of X_k for $1 \leq k \leq L-1$. The final gray dilation and erosion of image X are calculated as

$$\mathrm{D}(\vec{u}) = \sum_{k=1}^{L-1} \mathrm{D}_k(\vec{u}),$$

$$\mathrm{E}(\vec{u}) = \sum_{k=1}^{L-1} \mathrm{E}_k(\vec{u})$$

for any $\vec{u} \in \mathbb{B}$.

Algorithm 2 (gray dilation and erosion):

1. Decompose X to the $\mathrm{X}_1, \mathrm{X}_2, \ldots, \mathrm{X}_{L-1}$.
2. Calculate $\mathrm{D}_1, \mathrm{D}_2, \ldots, \mathrm{D}_{L-1}$ and $\mathrm{E}_1, \mathrm{E}_2, \ldots, \mathrm{E}_{L-1}$ via algorithm 1.
3. Summarize $\mathrm{D}(\vec{u}) = \sum_{k=1}^{L-1} \mathrm{D}_k(\vec{u})$.
4. Summarize $\mathrm{E}(\vec{u}) = \sum_{k=1}^{L-1} \mathrm{E}_k(\vec{u})$.

The time complexity of algorithm 2 is $\mathrm{T}(N, L) \sim (L-1) N \log N$, which is proportional to the number of gray levels. It implies that the algorithm 2 is faster than the traditional gray dilation for the mask size $m \geq \lambda(L-1) \log N$.

4 Dilation with Spherical Mask

It is very difficult to approximate spherical mask in the rectangular domain $\mathbb{B}$ but the algorithms 1, 2 only operate with Fourier spectrum $\mathcal{M}(\vec{\omega})$ of given mask M. Any spherical mask of radius $R > 0$ is defined as

$$\mathrm{M}(\vec{w}) = \begin{cases} 1 & \text{for } ||\vec{w}||_2 \leq R \\ 0 & \text{otherwise} \end{cases}$$

for $\vec{w} \in \mathbb{Z}^n$ in the discrete case. After the extension to the real case ($\vec{w} \in \mathbb{R}^n$) and Fourier transform, we obtain:

$$\mathcal{M}(\vec{\omega}) = \frac{2\sin R\omega}{\omega} \qquad \text{for } n = 1$$
$$\mathcal{M}(\vec{\omega}) = \frac{2\pi R \mathrm{J}_1(R\omega)}{\omega} \qquad \text{for } n = 2$$
$$\mathcal{M}(\vec{\omega}) = \frac{4\pi(\sin R\omega - R\omega\cos R\omega)}{\omega^3} \qquad \text{for } n = 3$$

where $\omega = ||\vec{\omega}||_2$ and J_1 is the Bessel function of the first kind.

The spectra of circle ($n = 2$) and sphere ($n = 2$) are useful for the realization of biomedical image gray morphology.

5 Experimental Part

The aim of experimental part is to verify the advantage of previous algorithms in the case of dilation and erosion with spherical masks.

5.1 Dilation and Erosion of Binary Image

The study was performed for $n \in \{2, 3\}$ and $N_1 = N_2 = N_3 = 128$. The analytical form of mask spectrum $\mathcal{M}(\vec{\omega})$ was sampled first. The referential discrete mask spectrum was obtained as FFT of discrete spherical mask $\mathrm{M}(\vec{w})$ denoted as $\mathcal{M}^*(\vec{\omega}) = \mathrm{FFT}(\mathrm{M}(\vec{w}))$. The algorithm 1 (binary form) was tested via dilation and erosion of circles ($r = 8.7$, $r = 16.3$), squares ($a = 19.6$, $a = 29$), and diamonds ($a = 13.86$, $a = 20.5$) for $n = 2$ and mask radii $R \in \{4.1, 8.5, 11.6\}$. Then, it was tested in 3-D via dilation and erosion of spheres ($r = 6.4$, $r = 9.7$, $r = 13.4$) and cubes ($a = 9.7$, $a = 13.4$, $a = 15.1$) for mask radii $R \in \{4.2, 7.7, 11.1\}$. The measures of dilated and eroded objects were calculated exactly and compared with measures from sampled analytical and discrete masks. The results are summarized in Tabs. 1–4.

5.2 Fuzzy Image Processing

Denoting erosion and dilation of image X as $\mathrm{E}(X)$ and $\mathrm{D}(X)$, we define *opening* as $\mathrm{O}(X) = \mathrm{D}(\mathrm{E}(X))$ and *closing* as $\mathrm{C}(X) = \mathrm{E}(\mathrm{D}(X))$. The *white top hat* is defined as $\mathrm{WTH}(X) = X - \mathrm{O}(X)$ and *black top hat* is defined as $\mathrm{BTH}(X) = \mathrm{C}(X) - X$. Then we can also define (for the given constant mask):

- *fuzzy edge detector*: $\mathrm{FED}(X) = \min(X - \mathrm{E}(X), \mathrm{D}(X) - X)$,
- *fuzzy Minkowski sausage*: $\mathrm{FMS}(X) = \mathrm{D}(X) - \mathrm{E}(X)$,
- *fuzzy filtering*: $\mathrm{FFI}(X) = (\mathrm{O}(\mathrm{C}(X)) + \mathrm{C}(\mathrm{O}(X)))/2$ and
- *fuzzy enhancement*: $\mathrm{FEH}(X) = \max\{X + \mathrm{WTH}(X) - \mathrm{BTH}(X), 0\}$.

Original 3-D gray SPECT image was padded with zeros to size $128 \times 128 \times 128$ with 201 gray levels (Fig. 1) was analyzed via gray level morphology with spherical mask of radius $R = 2.5$. The results of various fuzzy-morphological operations (based on gray dilation and erosion) are demonstrated on horizontal slice of index 60. The results of fuzzy operations mentioned above are depicted in Figs. 2–5.

6 Conclusion

The morphological operation (like dilation and erosion) of binary and gray level images with large spherical mask can be realized using the fast Fourier transform. Our method is based on the gray level image decomposition to binary images, their processing via the FFT, nonlinear threshold and composition to the final gray image. In the case of spherical mask, the mask radius can have non-integer value. This is an advantage for the sampled analytical solution. The integer radius of mask can cause worse results comparing to that achieved using the analytical approach. Its approximation in Fourier domain decreases the discretization error of resulting dilated or eroded images. The main advantage of our method is the independence on the mask size at the time complexity of morphological operations depends only on the image size. It will enable to use large masks for fractal analysis in our future work.

References

[1] Basart, J. P., Chacklackal, M. S., and Gonzales, R. C.: Introduction to Gray-Scale Morphology. In: *Advances in Image Analysis*, Y. Mahdavieh and R. C. Gonzales (eds.), SPIE Press, Bellingham, Wash., pp. 306–354, 1992.

[2] Giardina, C. R., and Dougherty, E. R.: *Morphological Methods in Image and Signal Processing*, Prentice Hall, Upper Saddle River, New Jersey, 1988.

[3] Gonzalez, R. C., Woods, R. E., and Eddins, S. L.: *Digital Image Processing using MATLAB*, Prentice Hall, 2004.

[4] Goutsias, J., Vincent, L., and Bloomberg, D. S.: *Mathematical Morphology and Its Application to Image and Signal Processing*, Kluwer Academic Publishers, Boston, Mass, 2000.

[5] Mitra, S. K., and Sicuranza, G. L.: *Nonlinear Image Processing*, Academic Press, London, 2001.

[6] Serra, J.: *Image Analysis and Mathematical Morphology*, Academic Press, New York, 1982.

			area			relative error [%]	
object	size	R	exact	sampled	discrete	sampled	discrete
circle	8.7	4.1	514.719	497.000	489.000	3.442	4.997
circle	8.7	8.5	929.409	905.000	897.000	2.626	3.487
circle	8.7	11.6	1294.619	1261.000	1253.000	2.597	3.215
circle	16.3	4.1	1307.405	1289.000	1273.000	1.408	2.632
circle	16.3	8.5	1932.205	1909.000	1901.000	1.201	1.615
circle	16.3	11.6	2445.447	2417.000	2409.000	1.163	1.490
square	9.8	4.1	758.410	697.000	697.000	8.097	8.097
square	9.8	8.5	1277.540	1157.000	1161.000	9.435	9.122
square	9.8	11.6	1716.333	1573.000	1573.000	8.351	8.351
square	14.5	4.1	1369.410	1337.000	1337.000	2.367	2.367
square	14.5	8.5	2053.980	1957.000	1961.000	4.722	4.527
square	14.5	11.6	2609.333	2493.000	2493.000	4.458	4.458
diamond	9.8	4.1	472.183	405.000	409.000	14.228	13.381
diamond	9.8	8.5	890.276	837.000	837.000	5.984	5.984
diamond	9.8	11.6	1257.884	1177.000	1177.000	6.430	6.430
diamond	14.5	4.1	809.610	745.000	749.000	7.980	7.486
diamond	14.5	8.5	1344.687	1317.000	1317.000	2.059	2.059
diamond	14.5	11.6	1794.716	1737.000	1737.000	3.216	3.216

Table 1: Binary 2-D dilation

object	size	R	area			relative error [%]	
			exact	sampled	discrete	sampled	discrete
circle	8.7	4.1	66.476	69.000	77.000	3.797	15.831
circle	8.7	8.5	0.126	1.000	1.000	695.775	695.775
circle	8.7	11.6	0.000	0.000	0.000	–	–
circle	16.3	4.1	467.595	489.000	501.000	4.578	7.144
circle	16.3	8.5	191.134	205.000	205.000	7.254	7.254
circle	16.3	11.6	69.398	69.000	73.000	0.573	5.191
square	9.8	4.1	129.960	121.000	121.000	6.894	6.894
square	9.8	8.5	6.760	9.000	9.000	33.136	33.136
square	9.8	11.6	0.000	0.000	0.000	–	–
square	14.5	4.1	432.640	441.000	441.000	1.932	1.932
square	14.5	8.5	144.000	169.000	169.000	17.361	17.361
square	14.5	11.6	33.640	49.000	49.000	45.660	45.660
diamond	9.8	4.1	32.028	37.000	41.000	15.525	28.015
diamond	9.8	8.5	0.000	0.000	0.000	–	–
diamond	9.8	11.6	0.000	0.000	0.000	–	–
diamond	14.5	4.1	151.440	177.000	181.000	16.878	19.519
diamond	14.5	8.5	12.293	13.000	13.000	5.754	5.754
diamond	14.5	11.6	0.000	0.000	0.000	–	–

Table 2: Binary 2-D erosion

object	size	R	area			relative error [%]	
			exact	sampled	discrete	sampled	discrete
sphere	6.4	4.2	4988.916	4577.000	4397.000	8.257	11.865
sphere	6.4	7.7	11742.105	11025.000	10851.000	6.107	7.589
sphere	6.4	11.1	22449.298	21487.000	21259.000	4.287	5.302
sphere	9.7	4.2	11249.495	11067.000	10731.000	1.622	4.609
sphere	9.7	7.7	22066.647	21679.000	21157.000	1.757	4.122
sphere	9.7	11.1	37694.554	37379.000	36761.000	0.837	2.477
sphere	13.4	4.2	22836.346	22263.000	21843.000	2.511	4.350
sphere	13.4	7.7	39349.206	38737.000	38017.000	1.556	3.386
sphere	13.4	11.1	61600.872	60767.000	60041.000	1.354	2.532
cube	9.7	4.2	20321.305	18167.000	17963.000	10.601	11.605
cube	9.7	7.7	37442.162	32817.000	32337.000	12.353	13.635
cube	9.7	11.1	60623.481	56041.000	54721.000	7.559	9.736
cube	13.4	4.2	42114.402	40879.000	40579.000	2.933	3.646
cube	13.4	7.7	69319.549	65033.000	64361.000	6.184	7.153
cube	13.4	11.1	103933.216	101553.000	99993.000	2.290	3.791
cube	15.1	4.2	55858.198	57083.000	56735.000	2.193	1.570
cube	15.1	7.7	88467.789	86853.000	86085.000	1.825	2.693
cube	15.1	11.1	129083.243	131245.000	129493.000	1.675	0.317

Table 3: Binary 3-D dilation

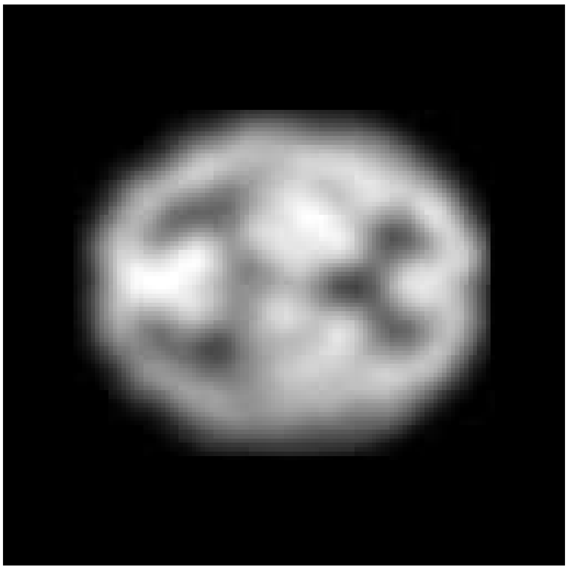

Figure 1: Original 3-D gray SPECT image

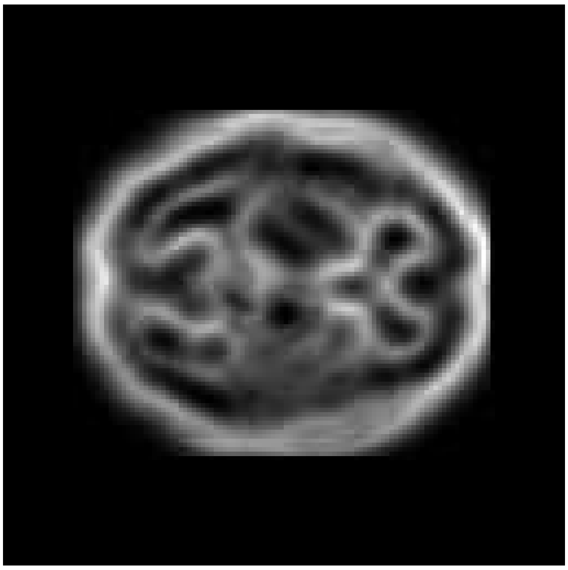

Figure 2: Fuzzy edge detector

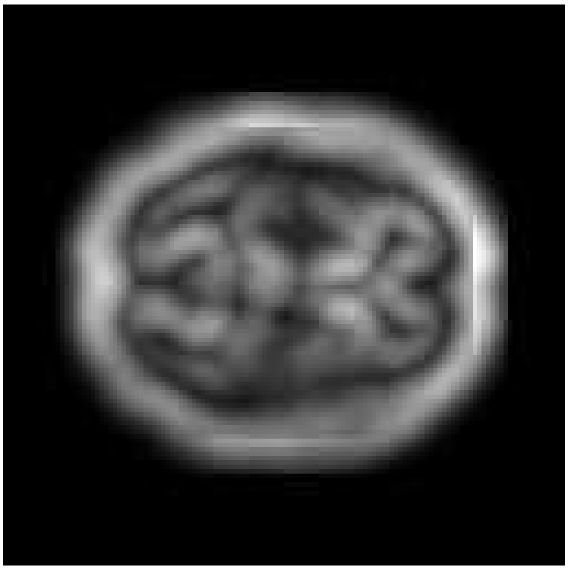

Figure 3: Fuzzy Minkowski sausage

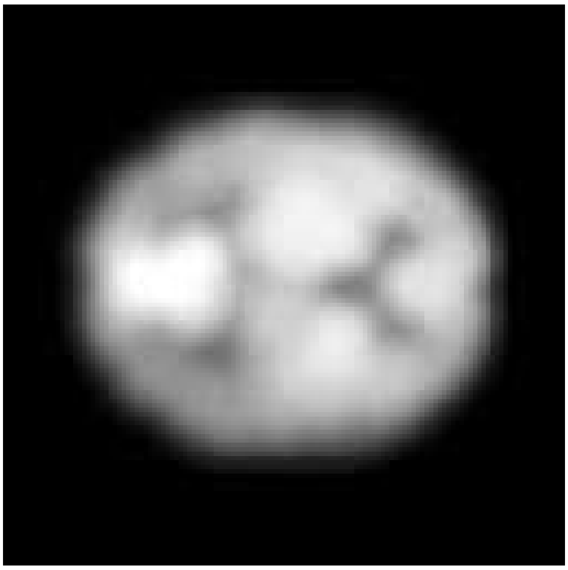

Figure 4: Fuzzy filtering

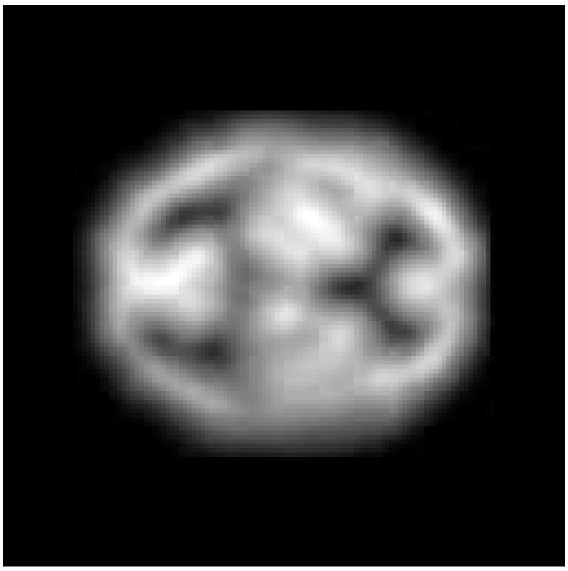

Figure 5: Fuzzy enhancement

			area			relative error [%]	
object	size	R	exact	sampled	discrete	sampled	discrete
sphere	6.4	4.2	44.602	33.000	57.000	26.013	27.796
sphere	6.4	7.7	0.000	0.000	0.000	–	–
sphere	6.4	11.1	0.000	0.000	0.000	–	–
sphere	9.7	4.2	696.910	739.000	775.000	6.040	11.205
sphere	9.7	7.7	33.510	15.000	33.000	55.238	1.523
sphere	9.7	11.1	0.000	0.000	0.000	–	–
sphere	13.4	4.2	3261.761	3335.000	3407.000	2.245	4.453
sphere	13.4	7.7	775.735	695.000	805.000	10.408	3.773
sphere	13.4	11.1	50.965	45.000	57.000	11.704	11.841
cube	9.7	4.2	1331.000	1287.000	1331.000	3.306	0.000
cube	9.7	7.7	64.000	69.000	125.000	7.813	95.313
cube	9.7	11.1	0.000	0.000	0.000	–	–
cube	13.4	4.2	6229.504	6851.000	6859.000	9.977	10.105
cube	13.4	7.7	1481.544	1893.000	2197.000	27.772	48.291
cube	13.4	11.1	97.336	105.000	125.000	7.874	28.421
cube	15.1	4.2	10360.232	12159.000	12167.000	17.362	17.439
cube	15.1	7.7	3241.792	4497.000	4913.000	38.720	51.552
cube	15.1	11.1	512.000	629.000	729.000	22.852	42.383

Table 4: Binary 3-D erosion

Jaromír Kukal
[1] Institute of Chemical Technology, Prague
Faculty of Chemical Engineering
Department of Computing and Control Engineering
Technická 5, 166 28 Prague 6 – Dejvice
[2] Czech Technical University in Prague
Faculty of Nuclear Sciences and Physical Engineering
Department of Software Engineering in Economy
Trojanova 13, 120 00 Prague 2
Phone: +420 224 358 583
E-mail: `Jaromir.Kukal@dc.fjfi.cvut.cz`

Dana Majerová
Czech Technical University in Prague
Faculty of Nuclear Sciences and Physical Engineering
Department of Software Engineering in Economy
Pohranicní 1288/1, 405 01 Decín 1
Phone: +420 224 358 481, fax: +420 412 512 730
E-mail: `Dana.Majerova@dc.fjfi.cvut.cz`

Aleš Procházka
Institute of Chemical Technology, Prague
Faculty of Chemical Engineering
Department of Computing and Control Engineering
Technická 5, 166 28 Prague 6 – Dejvice
Phone: +420 224 354 170, fax: +420 224 355 053
E-mail: `A.Prochazka@ieee.org`
WWW address: `http://dsp.vscht.cz/`